Crystal structure of 3,3′-(E)-diazene-1,2-diylbis{4-[(3,4-dinitro-1H-pyrazol-1-yl)-NNO-azoxy]-1,2,5-oxadiazole}

A. O. Dmitrienko,[1,a)] A. A. Konnov,[2] and M. S. Klenov[2]

[1] *Department of Chemistry, M. V. Lomonosov Moscow State University, Leninskie Gory, 119991 Moscow, Russian Federation*

[2] *N. D. Zelinsky Institute of Organic Chemistry Russian Academy of Sciences, Leninsky Prosp. 47, 119991 Moscow, Russian Federation*

(Received 3 September 2020; accepted 20 January 2021)

The crystal structure of a novel high-energy density material 3,3′-(E)diazene-1,2-diylbis{4-[(3,4-dinitro-1H-pyrazol-1-yl)-NNO-azoxy]-1,2,5-oxadiazole} ($C_{10}H_2N_{18}O_{12}$) was determined and refined using laboratory powder diffraction data. The title compound crystallizes in space group $P2_1/c$ with $a = 9.5089(3)$ Å, $b = 11.6331(4)$ Å, $c = 10.6270(3)$ Å, $\beta = 116.2370(12)$, $V = 1054.43(6)$ Å^3. The asymmetric unit contains half of the molecule. The molecular conformation contains a weak intramolecular hydrogen bond C–H⋯O–N, both nitro groups are disordered, and the structure is dominated by weak O⋯π and O⋯O contacts. © *The Author(s), 2021. Published by Cambridge University Press on behalf of International Centre for Diffraction Data.*
[doi:10.1017/S0885715621000208]

Key words: Rietveld refinement, DFT calculations, high-energy density materials

I. INTRODUCTION

X-ray powder diffraction techniques are routinely used in analysis of high-energy density materials. Their main objectives are phase analysis and the calculation of crystal density at room temperature. When single-crystal experiments are unavailable, they are also used to determine the crystal structure (and thus confirm the molecular structure) (Klenov *et al.*, 2016).

High-energy density materials (HEDMs) containing azoxy groups are a subject of intensive research (Fischer *et al.*, 2014; Yu *et al.*, 2015; Liu *et al.*, 2016). However, only few (and not high-energy) compounds with an azoxy group bonded to a nitrogen atom of a heterocycle were reported (Moriarty *et al.*, 1990; Semenov *et al.*, 1992). Additional N–N bonds can increase the enthalpy of formation and thus energy density. A two-dimentional molecular diagram for 3,3′-(E)-diazene1,2-diylbis{4-[(3,4-dinitro-1H-pyrazol-1-yl)-NNO-azoxy]-1,2,5-oxadiazole} ($C_{10}H_2N_{18}O_{12}$) is shown in Figure 1.

II. EXPERIMENTAL

A. Safety precautions

Although we have encountered no difficulties during the preparation and handling of compound described in this paper, it is potentially explosive energetic material which is sensitive to impact and friction. Mechanical actions of this energetic material, involving scratching or scraping, must be avoided. Any manipulations must be carried out by using appropriate standard safety precautions (face shield, ear protection, body armor, Kevlar® gloves, and grounded equipment).

3,3′-(E)-Diazene-1,2-diylbis{4-[(3,4-dinitro-1H-pyrazol-1-yl)-NNO-azoxy]1,2,5-oxadiazole} was synthesized in three steps from known 1-amino-3,4-dinitropyrazole (Yin *et al.*, 2014) as part of Russian Science Foundation project 19-13-00276.

The compound is an impact and friction sensitive explosive, so caution is needed during sample preparation. The sample was ground in agate mortar in small (~5 mg) portions and placed between two Kapton films with a PTFE spatula.

The powder pattern was measured on a Bruker AXS D8 Advance Vario X-ray powder diffractometer equipped with a primary monochromator (Cu$K\alpha_1$, $\lambda = 1.54056$ Å) and 1D LynxEye PSD. Data were collected at room temperature in the range 6–90° 2θ with a 0.01° 2θ step size in the transmission mode (Figure 2).

The diffraction pattern was indexed on a primitive monoclinic cell with $a = 9.5089(3)$ Å, $b = 11.6331(4)$ Å, $c = 10.6270(3)$ Å, $\beta = 116.2370(12)$ using the SVD (singular value decomposition) index algorithm (Coelho, 2003) as implemented in Bruker TOPAS 5.0 (Coelho, 2018), and space group determination was carried out using statistical systematic absences analysis as implemented in ExtSym (Markvardsen *et al.*, 2008). The resulting most probable space group $P2_1/c$ was later confirmed by structure solution and refinement.

Parallel tempering, as implemented in FOX (Favre-Nicolin and Černý, 2002), was used to solve the crystal structure in direct space. The Rietveld refinement (with Bruker TOPAS 5.0) was carried out using bond and angle restraints derived from periodic dispersion-corrected density functional theory (PW-DFT-D) calculations and a "riding" model for hydrogen atom. Restraint weight was automatically decreased during the refinement, and refinement result of more restrained model served as a starting structure for the next less restrained

---

[a)] Author to whom correspondence should be addressed. Electronic mail: dmitrienka@gmail.com

0885-7156/2021/36(2)/134/6/$18.00

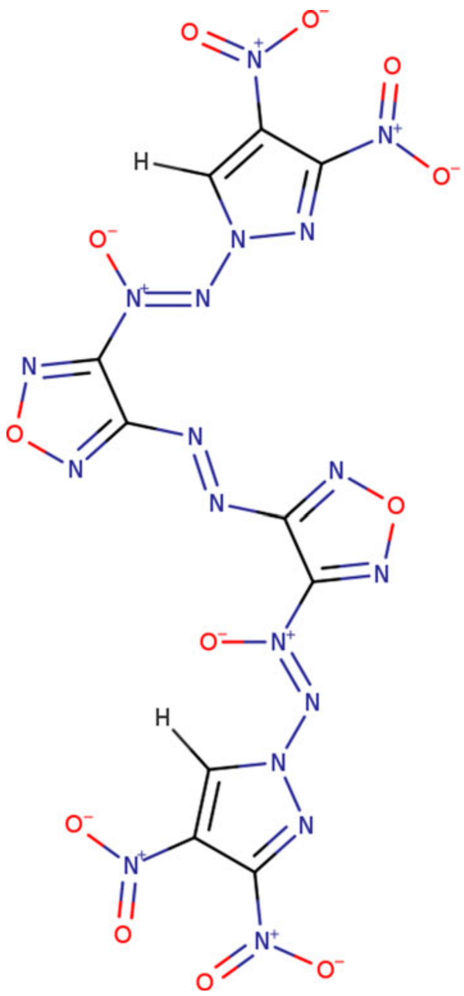

Figure 1. Molecular structure of the 3,3′-(E)-diazene-1,2-diylbis{4-[(3,4dinitro-1H-pyrazol-1-yl)-NNO-azoxy]-1,2,5-oxadiazole}.

one. For detailed explanation of the methodology, see Dmitrienko and Bushmarinov (2015).

PW-DFT-D calculations were performed in VASP 5.4.4 (Kresse and Hafner, 1993, 1994; Kresse and Furthmüller, 1996a, 1996b) using the PBE functional (Perdew *et al.*, 1996) corrected by Grimme D3 van der Waals correction (Grimme *et al.*, 2010) with Becke-Jonson damping (Grimme *et al.*, 2011). A plane-wave basis set with "normal" projector augmented wave (PAW) pseudopotentials (Blöchl, 1994; Kresse and Joubert, 1999) as supplied with VASP was employed. All optimizations were performed using energy cutoff of 600 eV. Default 0.5 $Å^{-1}$ *k*-point mesh and 8 *k*-points were used in all calculations.

Root-mean-square (rms) Cartesian displacement between the Rietveld refined structure and the PW-DFT-D optimized ones were calculated as suggested by Neumann (van de Streek and Neumann, 2014).

III. RESULTS AND DISCUSSION

The cell and molecular volume indicate $Z' = 1/2$. Parallel tempering runs in FOX lead to two global minimization solutions with almost identical χ^2; views of their asymmetric units are shown on Figures 3 and 4. The only difference between the structures is the mutual arrangement of C-H and N-lone pair fragments of the pyrazole ring.

It is difficult to distinguish two 7 electron fragments given only diffraction data, but it can often be done by analyzing intermolecular contacts. Structure **2** contains highly unusual contact C-H⋯π with furazan ring with H⋯O distance of 2.09 Å (Figure 5). The shortest H⋯$O_{aromatic}$ distance (with normalized C-H bond length) in the Cambridge Structural Database (CSD) is 2.15 Å and only 10 structures has H⋯O distance less than 2.3 Å. None of them are C-H⋯π interactions: the C-H bonds in all of them are almost parallel to the ring planes. It is unlikely that the structure contains such unprecedented contact; we should prefer structure **1**.

As an additional evidence, structures **1** and **2** were energy-optimized with PW-DFT-D in VASP with both fixed and free unit cell and the energies were compared. For structure **1**, PW-DFT-D optimized energies are −603.410/−603.446 eV for fixed/relaxed cell calculations. For structure **2**, optimized energies are −601.852/−601.979 eV. So structure **1** is more than 8 kcal/mol more energetically favorable.

Rietveld refinement was performed with fixed-cell energy-optimized structure **1** as source of bond and angle restraints. The N1O1O2 group got distorted during the refinement and thermal parameters for O1 and O2 became large

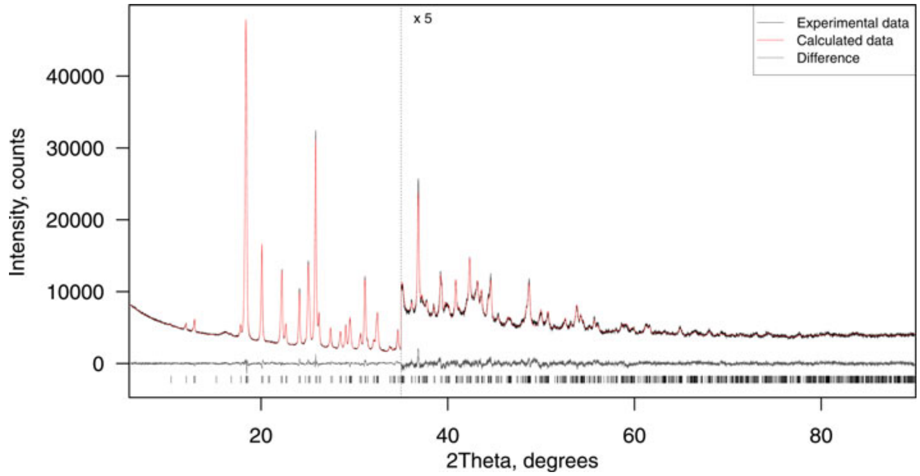

Figure 2. Final observed (black), calculated (red) and difference profiles for the Rietveld refinement.

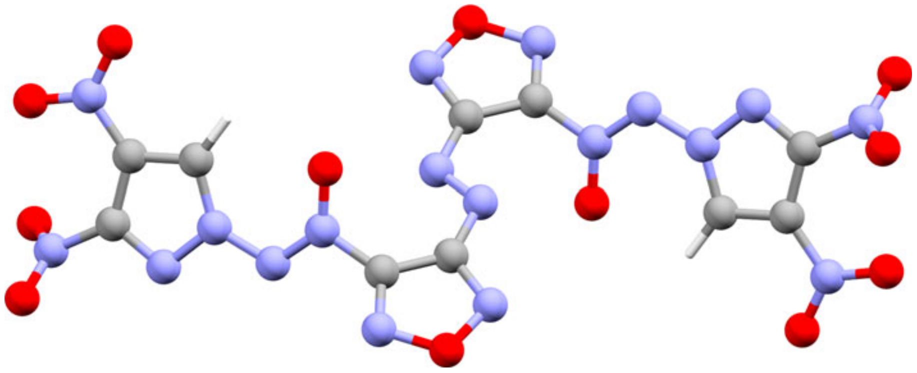

Figure 3. General view of **1** in a crystal.

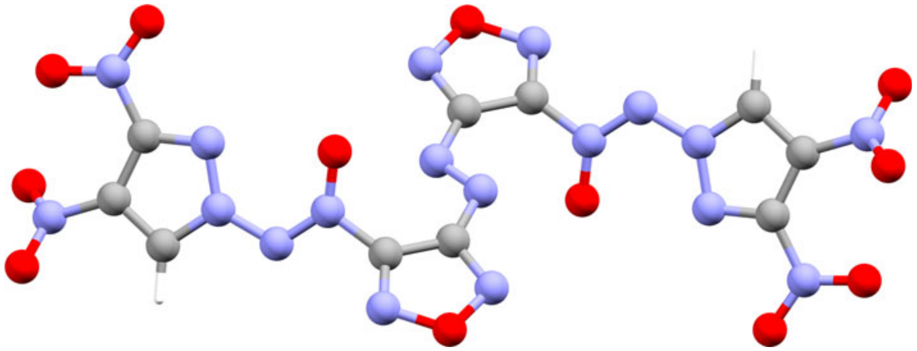

Figure 4. General view of **2** in a crystal.

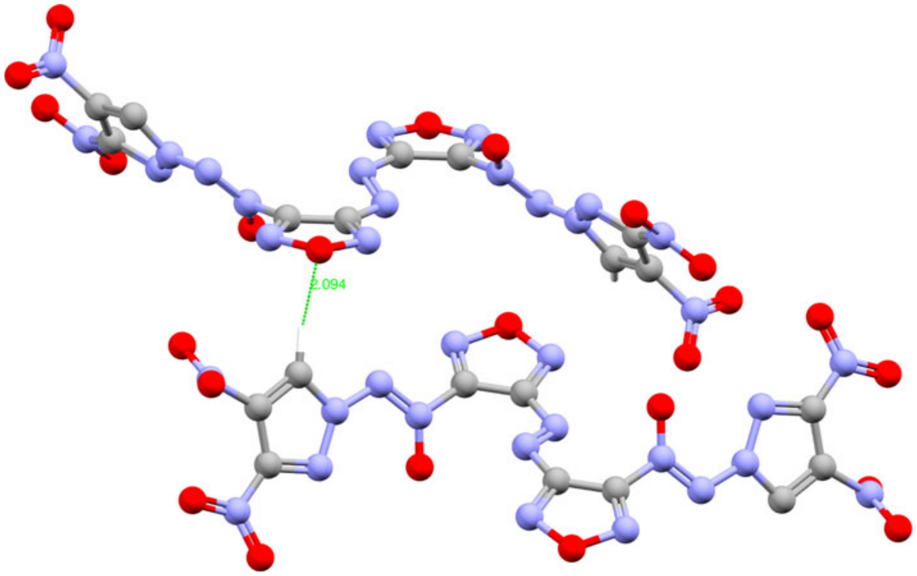

Figure 5. Unusual contact in structure **2.**

when refined independently. A CSD search showed several hundreds of disordered nitro groups. So, we constructed and refined a disordered model; the occupancy of the minor component was close to 0.33. Even though no issues were found with distortion or thermal parameters of the second nitro group we added its minor component to the model to prevent short O···O contacts. That did not improve the *R* factors though. Final refinement with 108 variables and 69 restraints over 8017 data points yielded $R_{\mathrm{p}}/R'_{\mathrm{p}}/R_{\mathrm{wp}}/R'_{\mathrm{wp}}/R_{\mathrm{Bragg}} = 2.18/8.17/2.94/7.45/0.91\%$, GOF = 1.44 and occupancy of the minor component 0.378(11) (Figure 6).

Powder data can give us very few hints about disorder details. To check if our model makes sense, we optimized the minor component with PW-DFTD (in addition to already optimized major component). For it PW-DFT-D optimized energies are −603.372/−603.400 eV for fixed/relaxed cell

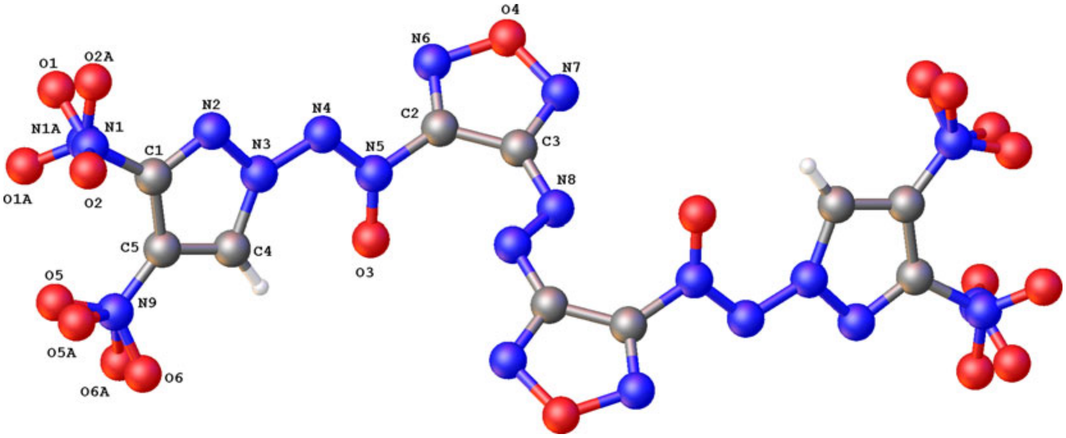

Figure 6. Final refined structure with atom numbering. The atoms are represented by 50% probability spheroids.

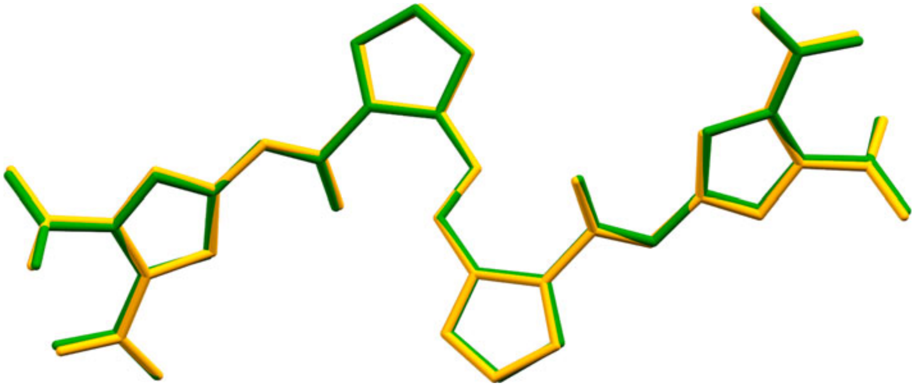

Figure 7. Comparison of energy-optimized (orange) and Rietveld refined (green) major component of the disordered structure.

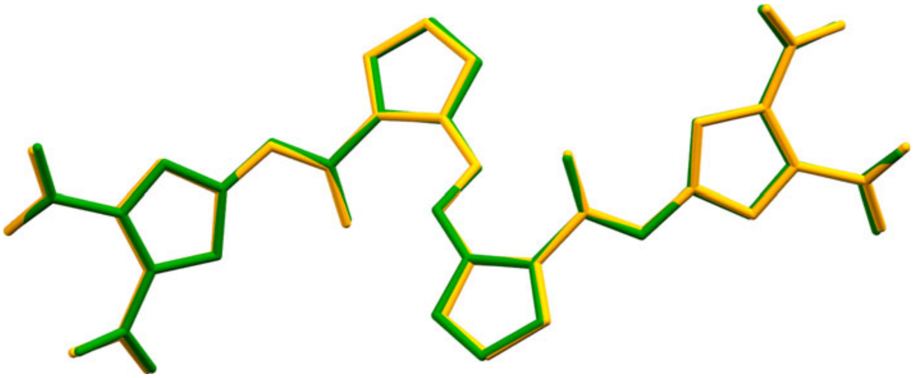

Figure 8. Comparison of energy-optimized (orange) and Rietveld refined (green) minor component of the disordered structure.

calculations. The energy difference between components is as small as 0.25 kcal/mol, which is expected.

The root mean Cartesian displacement between free-cell energy-optimized structure and final Rietveld refined structure is 0.11 Å for the major component and 0.09 Å for the minor component, which is within the range expected for correct structures. Comparison of the final Rietveld refined structure with fixed-cell energy-minimized structures of major and minor components are shown on Figures 7 and 8.

Figure 9 depicts the packing of **1**. The shortest intermolecular contact in the structure is O···π interaction between the nitro group and the furozan cycle with O···O distance 2.769 Å. The only hydrogen atom participates in a weak C-H···O hydrogen bond with the azoxy group (C···O distance is 3.228 Å). Other notable contacts are $NO_2\cdots O_2N$ (O···O distance is 3.154 Å) and $NO_2\cdots ONN$ (O···O distance is 3.134 Å). Lack of strong intermolecular interactions is typical for HEDMs.

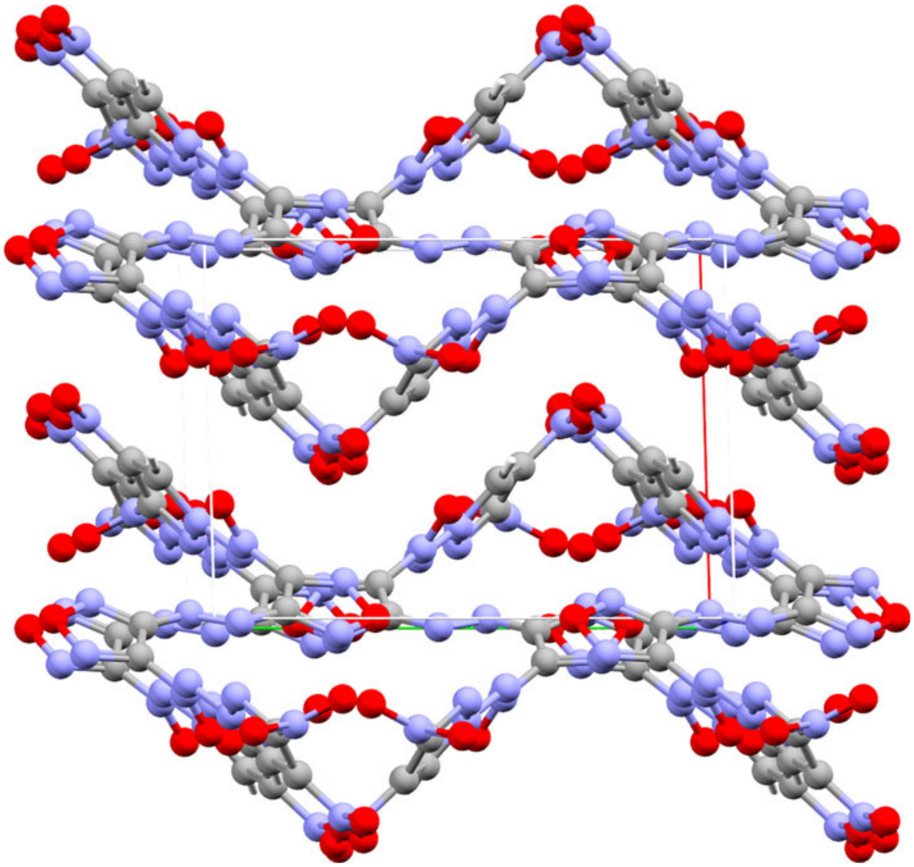

Figure 9. Fragment of the crystal packing of **1** (view along the *c* axis).

IV. DEPOSITED DATA

The Crystallographic Information File (ak1696.cif) which contains the results of the Rietveld Refinement and the raw powder diffraction pattern, and six files (VASP_1_major_refined_cell.cif, VASP_1_minor_fixed_cell.cif, VASP_1_minor_refined_cell.cif, VASP_2_fixed_cell.cif, VASP_2_refined_cell.cif) related to the PW-DFT-D calculations using VASP were deposited with ICDD. The VASP files were used to obtain the bond length and angle restraints for structures **1** and **2**, as discussed the EXPERIMENTAL section of this paper. These data files can be requested at info@icdd.com. The first file is also available from CCDC 2026495.

ACKNOWLEDGEMENTS

The study was funded by RFBR according to the research project № 1933-60075. M.S. Klenov and A. A. Konnov acknowledge financial support from Russian Science Foundation (project 19-13-00276) for the synthesis of the title compound. The *in crystal* calculations were carried out using the equipment of the shared research facilities of HPC computing resources at Lomonosov Moscow State University (Sadovnichy *et al.*, 2013).

Blöchl, P. E. (**1994**). “Projector augmented-wave method,” Phys. Rev. B **50**(24), 17953–17979.

Coelho, A. A. (**2003**). “Indexing of powder diffraction patterns by iterative use of singular value decomposition,” J. Appl. Crystallogr. **36**(1), 86–95.

Coelho, A. A. (**2018**). “Topas and topas-academic: an optimization program integrating computer algebra and crystallographic objects written in C++,” J. Appl. Crystallogr. **51**(1), 210–218.

Dmitrienko, A. O. and Bushmarinov, I. S. (**2015**). “Reliable structural data from Rietveld refinements via restraint consistency,” J. Appl. Crystallogr. **48**(6), 1777–1784.

Favre-Nicolin, V. and Černý, R. (**2002**). “FOX, ’free objects for crystallography’: a modular approach to *ab initio* structure determination from powder diffraction,” J. Appl. Crystallogr. **35**(6), 734–743.

Fischer, D., Klapötke, T. M., Reymann, M., and Stierstorfer, J. (**2014**). “Dense energetic nitraminofurazanes,” Chemistry **20**(21), 6401–6411.

Grimme, S., Antony, J., Ehrlich, S., and Krieg, H. (**2010**). “A consistent and accurate ab initio parametrization of density functional dispersion correction (DFT-d) for the 94 elements H-Pu,” J. Chem. Phys. **132**(15), 154104.

Grimme, S., Ehrlich, S., and Goerigk, L. (**2011**). “Effect of the damping function in dispersion corrected density functional theory,” J. Comput. Chem. **32**(7), 1456–1465.

Klenov, M. S., Anikin, O. V., Guskov, A. A., Churakov, A. M., Strelenko, Y. A., Ananyev, I. V., Bushmarinov, I. S., Dmitrienko, A. O., Lyssenko, K. A., and Tartakovsky, V. A. (**2016**). “Serendipitous synthesis of (tert-butyl-NNO-azoxy)acetonitrile: reduction of an oxime moiety to a methylene unit,” Eur. J. Org. Chem. **2016**(22), 3845–3855.

Kresse, G. and Furthmüller, J. (**1996a**). “Efficiency of ab-initio total energy calculations for metals and semiconductors using a plane-wave basis set,” Comput. Mater. Sci. **6**(1), 15–50.

Kresse, G. and Furthmüller, J. (**1996b**). “Efficient iterative schemes for ab initio total energy calculations using a plane-wave basis set,” Phys. Rev. B **54**(16), 11169–11186.

Kresse, G. and Hafner, J. (**1993**). “Ab initio molecular dynamics for liquid metals,” Phys. Rev. B **47**(1), 558–561.

Kresse, G. and Hafner, J. (**1994**). “Ab initio molecular-dynamics simulation of the liquid-metal–amorphous-semiconductor transition in germanium,” Phys. Rev. B **49**(20), 14251–14269.

Kresse, G. and Joubert, D. (**1999**). “From ultrasoft pseudopotentials to the projector augmented-wave method,” Phys. Rev. B **59**(3), 1758–1775.

Liu, Y., Zhang, J., Wang, K., Li, J., Zhang, Q., and Shreeve, J. (**2016**). "Bis(4-nitraminofurazanyl-3-azoxy)azofurazan and derivatives: 1,2,5-oxadiazole structures and high-performance energetic materials," Angew. Chem. Int. Ed. **55**(38), 11548–11551.

Markvardsen, A. J., Shankland, K., David, W. I. F., Johnston, J. C., Ibberson, R. M., Tucker, M., Nowell, H., and Griffin, T. (**2008**). "ExtSym: a program to aid space-group determination from powder diffraction data," J. Appl. Crystallogr. **41**(6), 1177–1181.

Moriarty, R. M., Hopkins, T. E., Prakash, I., Vaid, B. K., and Vaid, R. K. (**1990**). "Hypervalent iodine oxidation of amines in the presence of nitroso compounds: a method for the preparation of unsymmetrically substituted azoxy compounds," Synth. Commun. **20**(15), 2353–2357.

Perdew, J. P., Burke, K., and Ernzerhof, M. (**1996**). "Generalized gradient approximation made simple," Phys. Rev. Lett. **77**(18), 3865–3868.

Sadovnichy, V., Tikhonravov, A., Voevodin, V., and Opanasenko, V. (**2013**). "'Lomonosov': supercomputing at Moscow State University," in *Contemporary High Performance Computing: From Petascale toward Exascale* (Chapman & Hall/CRC Computational Science, Boca Raton, USA), pp. 283–307.

Semenov, S. E., Churakov, A. M., Chertanova, L. F., Strelenko, Y. A., Ioffe, S. L., and Tartakovskii, V. A. (**1992**). "Synthesis of 1-(2,4,6-trichlorophenyl)2-(1,2,4-triazol-4-yl)-diazene-1-oxide," Bull. Russ. Acad. Sci. Div. Chem. Sci. **41**(2), 277–279.

van de Streek, J., and Neumann, M. A. (**2014**). "Validation of molecular crystal structures from powder diffraction data with dispersion-corrected density functional theory (DFT-d)," Acta Crystallogr. B: Struct. Sci., Cryst. Eng. Mater. **70**(6), 1020–1032.

Yin, P., Zhang, J., He, C., Parrish, D. A., and Shreeve, J. M. (**2014**). "Polynitro-substituted pyrazoles and triazoles as potential energetic materials and oxidizers," J. Mater. Chem. A **2**, 3200–3208.

Yu, Q., Wang, Z., Yang, H., Wu, B., Lin, Q., Ju, X., Lu, C., and Cheng, G. (**2015**). "N-trinitroethyl-substituted azoxyfurazan: high detonation performance energetic materials," RSC Adv. **5**(35), 27305–27312.